THE JOURNAL OF BIOLOGICAL CHEMISTRY VOL. 282, NO. 48, pp. 35279–35292, November 30, 2007
Printed in the U.S.A.

A Subpopulation of Macrophages Infiltrates Hypertrophic Adipose Tissue and Is Activated by Free Fatty Acids via Toll-like Receptors 2 and 4 and JNK-dependent Pathways*[S]

Received for publication, August 14, 2007 Published, JBC Papers in Press, October 4, 2007, DOI 10.1074/jbc.M706762200

M. T. Audrey Nguyen[‡1], Svetlana Favelyukis[‡], Anh-Khoi Nguyen[‡], Donna Reichart[§], Peter A. Scott[¶], Alan Jenn[‡], Ru Liu-Bryan[¶], Christopher K. Glass[§], Jaap G. Neels[‡], and Jerrold M. Olefsky[‡]

From the [‡]Division of Endocrinology-Metabolism, the [§]Department of Cellular and Molecular Medicine, and the [¶]Veterans Affairs Medical Center, University of California, San Diego, La Jolla, California 92093

Obesity and type 2 diabetes are characterized by decreased insulin sensitivity, elevated concentrations of free fatty acids (FFAs), and increased macrophage infiltration in adipose tissue (AT). Here, we show that FFAs can cause activation of RAW264.7 cells primarily via the JNK signaling cascade and that TLR2 and TLR4 are upstream of JNK and help transduce FFA proinflammatory signals. We also demonstrate that F4/80$^+$CD11b$^+$CD11c$^+$ bone marrow-derived dendritic cells (BMDCs) have heightened proinflammatory activity compared with F4/80$^+$CD11b$^+$CD11c$^-$ bone marrow-derived macrophages and that the proinflammatory activity and JNK phosphorylation of BMDCs, but not bone marrow-derived macrophages, was further increased by FFA treatment. F4/80$^+$CD11b$^+$CD11c$^+$ cells were found in AT, and the proportion and number of these cells in AT is increased in ob/ob mice and by feeding wild type mice a high fat diet for 1 and 12 weeks. AT F4/80$^+$CD11b$^+$CD11c$^+$ cells express increased inflammatory markers compared with F4/80$^+$CD11b$^+$CD11c$^-$ cells, and FFA treatment increased inflammatory responses in these cells. In addition, we found that CD11c expression is increased in skeletal muscle of high fat diet-fed mice and that conditioned medium from FFA-treated wild type BMDCs, but not TLR2/4 DKO BMDCs, can induce insulin resistance in L6 myotubes. Together our results show that FFAs can activate CD11c$^+$ myeloid proinflammatory cells via TLR2/4 and JNK signaling pathways, thereby promoting inflammation and subsequent cellular insulin resistance.

Chronic inflammation is a well described feature of insulin resistance and obesity characterized by elevated proinflammatory JNK[2] and IKKβ kinase activity (1, 2) and increased cyto/chemokine expression in insulin target tissues (3). In white adipose tissue, chronic inflammation is associated with an increase in macrophage infiltration (4–6). Surgically induced weight loss (7), diet and exercise (8), and treatment with rosiglitazone, an insulin-sensitizing drug (5), all reduce macrophage infiltration in white adipose tissue (AT) and decrease the expression of proinflammatory markers in white AT and plasma. A definitive role for immune cells in metabolic dysregulation was recently demonstrated in mice with myeloid cell-specific knock-out of IKKβ (9), indicating that macrophage activation can cause systemic insulin resistance.

Macrophages are a heterogeneous population of phagocytic cells found throughout the body that originate from the mononuclear phagocytic system (10). These are highly plastic cells that arise from circulating myeloid-derived blood monocytes that have entered target tissues and gained the phenotypic and functional attributes of their tissue of residence. Like for other immune cells, the distribution and function of tissue macrophages have been largely characterized using monoclonal antibodies to cell surface proteins. In mice, the most commonly used monocyte/macrophage and myeloid cell surface markers are F4/80 and CD11b, although F4/80 and CD11b antibodies have been reported to react with eosinophils and dendritic cells and NK and other T and B cell subtypes, respectively (11).

In AT, resident macrophages are surrounded by adipocytes that constantly release free fatty acids (FFAs) via lipolysis. FFAs thus have the potential to activate AT macrophages and consequently alter their function. FFAs can cause activation of JNK and IKKβ inflammatory pathways in adipose tissue, liver, and skeletal muscle (1, 2, 12, 13), leading to cellular inflammation and insulin resistance. In man, elevated FFA levels are a feature of obesity and type 2 diabetes (12, 14). In animal models, high fat (HF) feeding and direct lipid infusion can increase plasma

* This work was supported by a University of California Discovery Biostar Grant and National Institutes of Health Grants DK33651 (to J. M. O.) and DK074868 (to C. K. G. and J. M. O.); the Fonds de la Recherche en Santé du Québec (to M. T. A. N.); National Institutes of Health Grant AR049416 (to R. L.-B.); and Scientist Development Grant 0635408N from the American Heart Association (to J. G. N.). The costs of publication of this article were defrayed in part by the payment of page charges. This article must therefore be hereby marked "*advertisement*" in accordance with 18 U.S.C. Section 1734 solely to indicate this fact.

[S] The on-line version of this article (available at http://www.jbc.org) contains supplemental Figs. S1–S3.

[1] To whom correspondance should be addressed: University of California, San Diego, 9500 Gilman Dr., La Jolla, CA 92093-0673. Fax: 858-534-6653; E-mail: m9nguyen@ucsd.edu.

[2] The abbreviations used are: JNK, c-Jun N-terminal kinase; FA, fatty acid; FFA, free fatty acid; TLR, Toll-like receptor; AT, adipose tissue; BM, bone marrow; BMDC, bone marrow-derived dendritic cell; BMDM, bone marrow-derived macrophage; HF, high fat; HFD, high fat diet; IL, interleukin; TNF, tumor necrosis factor; FBS, fetal bovine serum; BSA, bovine serum albumin; RT, reverse transcription; ELISA, enzyme-linked immunosorbent assay; siRNA, small interfering RNA; WT, wild type; GM-CSF, granulocyte macrophage-colony-stimulating factor; FACS, fluorescence-activated cell sorter; PBS, phosphate-buffered saline; ITT, insulin tolerance test; SVF, stromal vascular fraction; SVC, stromal vascular cell; NC, normal chow; MNC, mononuclear cells; CM, conditioned medium; KD, knockdown; qPCR, quantitative PCR.

FFA levels and cause tissue and systemic inflammation and insulin resistance (15, 16). Toll-like receptors (TLRs) are thought to participate in sensing extracellular FFAs. TLRs belong to the Toll/interleukin-1 receptor superfamily and are widely expressed on cells of the immune system (17, 18). TLRs recognize bacteria-associated molecular patterns with high specificity, and TLR-mediated signal transduction leads to the activation of JNK and NFκB signaling pathways (17, 19), initiating the innate immune response. The saturated FA, lauric acid, was shown to activate TLR2 in 293T cells as well as NFκB-mediated, TLR4-dependent signaling pathways in RAW264.7 cells (20). Similarly, an oleate/palmitate mixture can induce NFκB-dependent TLR4 signaling in 293T cells and cause inflammation in wild type (WT) but not TLR4-deficient adipocytes. The saturated FA palmitate was also shown to cause TLR4-dependent IκBα degradation in elicited peritoneal macrophages (21).

In the present study, we examined the effects of saturated and unsaturated FFAs in cultured RAW264.7 cells, primary bone marrow (BM)-derived cells and adipose tissue macrophages. We demonstrate that FFAs signal through both TLR2 and TLR4 to activate JNK and stimulate inflammatory pathways in CD11c$^+$ myeloid cells. We also show that in AT, F4/80$^+$CD11b$^+$CD11c$^+$ cells are the direct targets for FFAs and that HF feeding increases the number of these cells in AT. As such, these results provide a novel mechanistic link between lipid metabolism, inflammation, and insulin resistance.

EXPERIMENTAL PROCEDURES

Reagents—Antibodies to IL-6, MCP-1,TNF-α, and horseradish peroxidase-linked secondary antibodies were purchased from Santa Cruz Biotechnology (Santa Cruz, CA), and all other antibodies were from Cell Signaling (Beverly, MA). Tissue culture reagents were purchased from Invitrogen and Hyclone (Logan, UT).

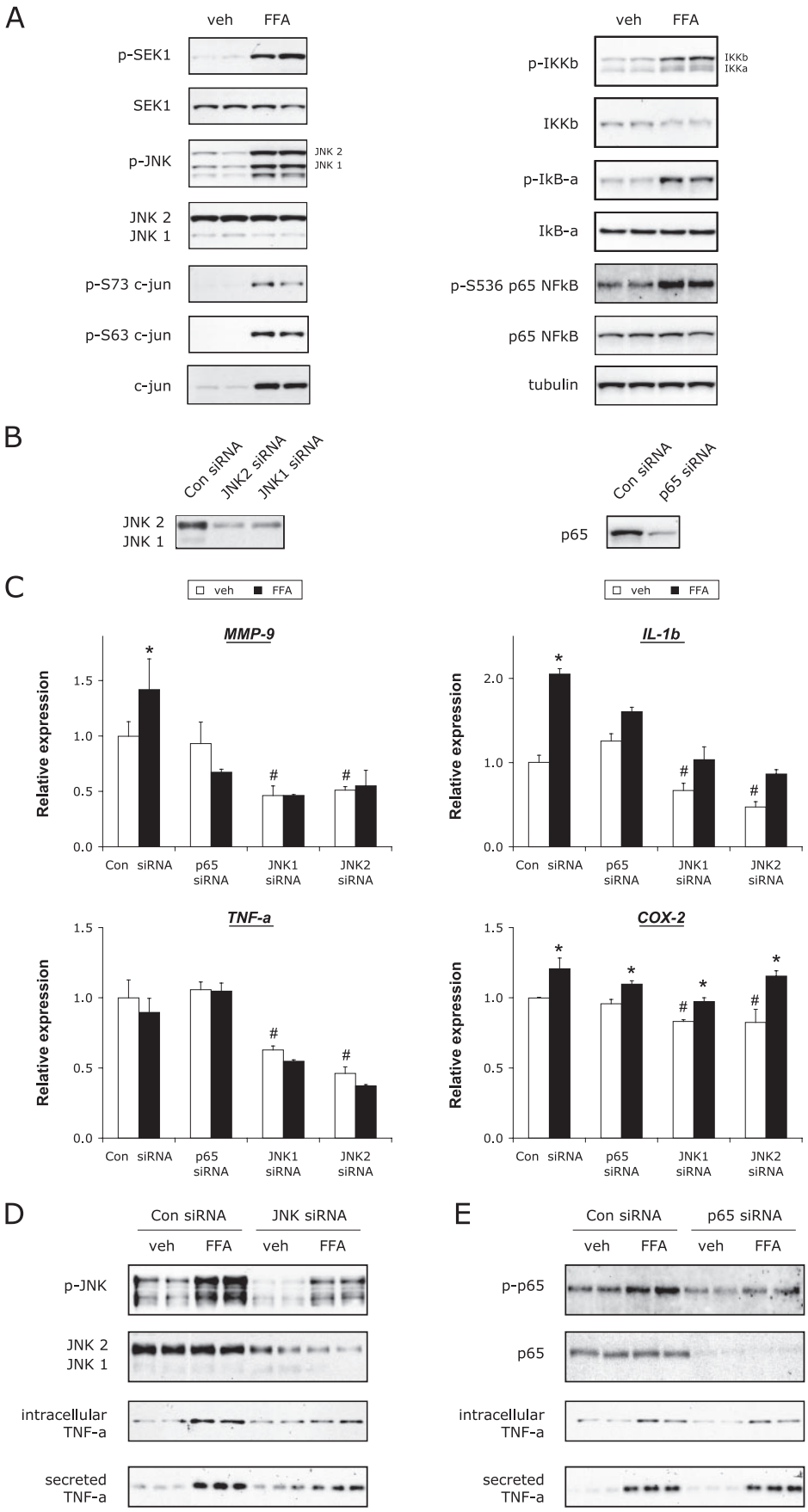

Cell Culture and Treatment—Mouse monocyte/macrophage RAW264.7 cells were obtained from American Type Culture Collection (Manassas, VA) and cultured in Dulbecco's modified Eagle's medium (1g/liter glucose) supplemented with 10% low endotoxin FBS. In pretreated cells, 1 μM rosiglitazone or vehicle Me_2SO was added at least 24 h prior to FFA treatment. RAW cells were then incubated for 3 h with either 500 μM of an FFA mixture containing equimolar amounts of tissue culture-grade arachidonic, lauric, linoleic, oleic, and myristic acids or with individual FFAs (500 μM) or ethanol vehicle in Dulbecco's modified Eagle's medium supplemented with FFA-free BSA (Sigma-Aldrich). All of the FFA solutions were pre-equilibrated with BSA at 37 °C for 1–1.5 h (22), and a 5:1 FFA:BSA ratio was used to simulate elevated FFAs levels.

We ensured that all components for cell culture and treatment experiments contained very low or undetectable amounts of contaminating lipopolysaccharide by measuring endotoxin levels in the serum, culture medium, BSA preparation, and FFA stock solutions (LAL assay kit, Cambrex, East Rutherford, NJ). All of the solutions used contained undetectable amounts of endotoxin except for the BSA solution, which contained 0.3 EU/ml (0.03 ng/ml) of endotoxin. This amount of contaminating lipopolysaccharide was not sufficient to activate RAW264.7 cells and BMDCs. We found that treating RAW264.7 cells and BMDCs with 0.03 ng/ml of endotoxin for 3 h did not cause phosphorylation of JNK and secretion of TNF-α and JNK phosphorylation in these cells (data not shown).

Western Blotting—The cells were lysed in cold buffer containing 50 mM HEPES, pH 7.4, 150 mM NaCl, 200 mM NaF, 20 mM sodium pyrophosphate, 10% glycerol, 1% Triton X-100, 4 mM sodium orthovanadate, 2 mM phenylmethylsulfonyl fluoride, and 1 mM EDTA. Whole cell lysates (25 μg) or conditioned medium (30 μl) were resolved by SDS-PAGE and transferred onto polyvinylidene difluoride membranes (Immobilon-P; Millipore, Bedford, MA). Following blocking with 5% milk in TBST, the membranes were probed with primary antibodies as indicated and subsequently incubated with horseradish peroxidase-linked secondary antibodies for chemiluminescent detection (Pierce). The blots were stripped in Restore^{TM} Western blot stripping buffer (Pierce) and reprobed as necessary.

Semi-quantitative RT-PCR—Total RNA was isolated and purified using RNeasy columns and RNase-free DNase according to the manufacturer's instructions (Qiagen). One-step RT-PCR kits (Qiagen) and sequence-specific primers (see supplemental Fig. S3) were used to generate RT-PCR products, which were then run on 8% acrylamide gels, stained with ethidium bromide, visualized, and quantitated using the Kodak ID Imaging station and software (Kodak Scientific Imaging Systems, New Haven, CT).

Real Time PCR—Total RNA was isolated from cells as outlined above. First strand cDNA was synthesized using SuperScript III and random hexamers (Invitrogen). The samples were run in 20-μl reactions using an AB1 7300 (Applied Biosystems, Foster City, CA); SYBR Green oligonucleotides were used for detection, and sequence-specific primers are listed in supplemental Fig. S3. Gene expression levels were calculated after normalization to the standard housekeeping gene *GAPDH* using the $\Delta\Delta C_T$ method as described by the manufacturer (Invitrogen) and expressed as relative mRNA levels compared with control.

ELISA—Conditioned medium was assayed for mouse IL-1β, IL-6, MCP-1, and TNF-α using ELISA kits (BIOSOURCE, Camarillo, CA) following the manufacturer's protocol.

Protein Knockdown—2×10^7 RAW264.7 cells were electroporated with 2.5 nmol of high pressure liquid chromatography-purified siRNA oligonucleotides (IDT, Coralville, IA) to mouse JNK1, JNK2, p65-NFκB, TLR2, or TLR4 or with luciferase control siRNA (oligonucleotide sequences in supplemental Fig. S3) using the XCell Gene Pulser (Bio-Rad). The cells were plated into 24-well tissue culture plates, and 24–48 h post-electroporation, they were treated with FFAs as described above. Conditioned medium and cell lysates were analyzed by immunoblotting.

Isolation and Treatment of Bone Marrow-derived Cells—All of the animal experiments were performed humanely under protocols approved by the University of California, San Diego. TLR2/4 DKO male mice on a C57BL/6 background (kindly provided by Dr. Shizuo Akira, University of Osaka, Japan) and WT C57BL/6 male mice were maintained under specific pathogen-free conditions.

Bone marrow cells were isolated from the femurs and tibias of 10–12-week-old homozygous and WT mice by flushing the medullary cavity with RPMI medium. After washing, the cells were seeded in tissue culture plates and differentiated into either bone marrow-derived macrophages (BMDMs) or bone marrow-derived dendritic cells (BMDCs) in RPMI medium containing 30% of L-929 conditioned medium or 10 or 40 ng/ml of recombinant GM-CSF, respectively, and supplemented with 20% low endotoxin FBS and streptomycin/penicillin. We observed that differentiating precursor cells in 40 ng/ml of GM-CSF yielded more BMDCs than when using 10 ng/ml of GM-CSF. However, this higher GM-CSF concentration did not affect BMDC proinflammatory gene expression (IL-6, TNF-α, IL-1β, and COX-2), differentiation and cell surface antigen

FIGURE 1. **FFAs activate JNK and IKKβ in RAW264.7 cells.** RAW264.7 cells were treated with 500 μM of a mixture of saturated and unsaturated FFAs or control vehicle (*veh*) for 3 h and analyzed as described. *A*, FFAs activate the JNK and IKKβ pathways in RAW264.7 cells. The cells were lysed for Western blot analysis of components of the JNK and IKK signaling pathways. $n = 6$ or more, in triplicate. *B–E*, contribution of the JNK and IKKβ-NFκB proinflammatory pathways in mediating the actions of FFAs. RAW264.7 cells electroporated with JNK1, JNK2, p65-NFκB, or control (*Con*) siRNAs were treated with 500 μM FFA or control vehicle (*veh*) for 3 h and harvested for real time qPCR and Western blot analyses. *B*, JNK isoforms and p65 protein were efficiently knocked down by RNA interference in RAW264.7 cells. *C–E*, JNK plays a more prominent role in mediating the effects of FFAs. *C*, effect of JNK and p65 KD on gene expression. JNK KD but not p65 KD decreased basal expression of MMP-9 gene by ~50%, of IL-1β and TNF-α genes by >40% and of COX-2 gene by ~20%. JNK KD and p65 KD also inhibited the FFA-induced increase in MMP-9 and IL-1β gene expression. *D* and *E*, effect of JNK and p65 KD on TNF-α protein levels. Both JNK and p65 KD decreased the ability of FFAs to activate JNK and p65, respectively, as assessed by JNK (*D*) and p65 (*E*) phosphorylation levels. JNK KD but not p65 KD can inhibit the FFA-induced increase in intracellular and secreted TNF-α levels. $n = 3$ or more in triplicate. *, $p < 0.05$ for FFA *versus* vehicle; #, $p < 0.05$ for vehicle *versus* control siRNA vehicle.

expression (F4/80, CD11b, and CD11c), as determined by qPCR and FACS analysis (data not shown). We were also able to differentiate BMDMs from bone marrow precursor cells using murine recombinant M-CSF (data not shown). BMDM and BMDC differentiation was complete 8 days after cell plating; this was confirmed by the expression of F4/80, a marker preferentially expressed by mature macrophages, and of CD11c, a cell surface marker for dendritic cells, using FACS (data not shown). For FFA experiments, day 8 or 9 BMDMs and BMDCs were stimulated with 500 μM FFA for 3 h, and conditioned medium and cell lysates were analyzed as indicated.

Immunohistocytochemistry—Paraffin-embedded adipose tissue was sectioned, deparaffinized, and rehydrated prior to endogenous peroxidase and biotin removal using 0.03% H_2O_2 and 0.1% avidin. The slides were heated in 0.1 M citrate buffer for antigen retrieval, cooled, washed, and then blocked with 1% BSA in TBST. The sections were incubated overnight with CD11c primary antibody (eBioscience, San Diego, CA). Biotin-conjugated secondary and horseradish peroxidase-conjugated streptavidin tertiary antibodies were applied for detection, and the sections were developed in substrate chromogen, counterstained in Mayers Hematoxylin, and mounted in Gelmount Biomedia.

Frozen quad muscle tissue was sectioned (5 um), air-dried, and fixed in acetone. After endogenous peroxidase removal using 0.03% H_2O_2, the sections were washed in PBS and blocked in 0.01% biotin for 15 min and then in 1% BSA in PBS for 30 min. Biotin-conjugated CD11c antibody was overlaid for 1 h, and the sections were further processed as outlined above.

Animal Studies—Wild type male C57BL/6 and *ob/ob*^{J} male mice were purchased from Harlan (Indianapolis, IN). The animals were housed in a pathogen-free facility with a 12-h light/12-h dark cycle and given free access to food and water. C57BL/6 mice were placed on a HFD consisting of 40% of calories from fat (TD.96132; Harlan Teklad, Madison, WI) starting at 12 weeks of age for 1, 12, or 20 weeks. Control C57BL/6 mice were fed a standard diet with 12% of calories from fat (LabDiet, 5001; Richmond, IN). The body weights and food intakes were recorded every week (data not shown).

An insulin tolerance test (ITT) was performed on mice after 1 and 12 weeks of chow or HFD feeding. The mice were fasted for 6 h. After 4 h of fasting, basal plasma glucose was measured. At 6 h, the mice were injected intraperitoneal with 0.6 units of insulin/kg of body weight. Blood glucose was measured through the tail tip at the indicated times, using a OneTouch glucose-monitoring system (Lifescan, Milpitas, CA).

Stromal Vascular Fraction (SVF) Isolation and FACS Analysis—Epididymal fat pads were excised from male C57BL/6 mice fed normal chow (NC) or HFD, weighed, rinsed three times in PBS, and then minced in FACS buffer (PBS + 1% low endotoxin BSA). Tissue suspensions were centrifuged at 500 × *g* for 5 min and then collagenase-treated (1 mg/ml; Sigma-Aldrich) for 30 min at 37 °C with shaking. The cell suspensions were filtered through a 100-μm filter and centrifuged at 500 × *g* for 5 min. SVF pellets were then incubated with RBC lysis buffer (eBioscience) for 5 min prior to centrifugation (300 × *g* for 5 min) and resuspension in FACS buffer.

Stromal vascular cells (SVCs) were incubated with Fc Block (BD Biosciences, San Jose, CA) for 20 min at 4 °C prior to staining with fluorescently labeled primary antibodies or control IgGs for 25 min at 4 °C. F4/80-allophycocyanin FACS antibody was purchased from AbD Serotec (Raleigh, NC); all other fluorescein isothiocyanate- and phycoerythrin-conjugated FACS antibodies were from BD Biosciences. The cells were gently washed twice and resuspended in FACS buffer with propidium iodide (Sigma-Aldrich). SVCs were analyzed using FACSCalibur and FACSAria flow cytometers (BD Biosciences). Unstained, single stains, and fluorescence minus one controls were used for setting compensation and gates.

For cell sorting, F4/80$^+$CD11b$^+$CD11c$^-$ and F4/80$^+$CD11b$^+$CD11c$^+$ cells from lean, NC SVFs were sorted into FBS. Sorted cells were allowed to recover for 2 h. The cells were then washed and treated with FFA for subsequent RNA extraction and real time PCR analysis.

Glucose Uptake Assay—BMDCs from WT and TLR2/4 DKO mice were treated with 500 μM FFA or vehicle for 3 h and then washed twice with RPMI medium to remove the FFAs. The cells were subsequently incubated with fresh culture medium containing 2% FBS. After 6 h of incubation, CM was harvested for ELISA analysis and co-culture experiments.

L6 myocytes were cultured in α-minimal essential medium supplemented with 10% FBS and differentiated into myotubes in α-minimal essential medium containing 2% FBS for ~6–7 days. The L6 myotube culture medium was then replaced with CM from BMDCs diluted 1:1 in fresh L6 differentiation medium. L6 myotubes were incubated with BMDC-derived CM for 24–48 h prior to assaying glucose uptake. For glucose uptake assays, L6 myotubes were serum starved for 3 h in α-minimal essential medium with 0.5% FFA-free BSA and then glucose-starved for 30 min in HEPES salt buffer containing 0.5% FFA-free BSA. The cells were stimulated with insulin (5 nM) at 37 °C for 20 min; tracer glucose was then added for 10 min. After 30 min of insulin stimulation, glucose uptake was assayed in quadruplicate wells for each condition using 1,2-^{3}H-2-deoxy-D-glucose (0.2 μCi, 0.1 mM, 10 min) in four independent experiments.

Data Analysis—Densitometric quantification and normalization were performed using the NIH Image 1.63 software. The values presented are expressed as the means ± S.E. The statistical significance of the differences between various treatments was determined by one-way analysis of variance with the Bonferroni correction.

RESULTS

FFAs Cause a Proinflammatory Response in RAW264.7 Cells—Recent studies suggest that chronic inflammation in AT is an important mechanism underlying the insulin resistance associated with obesity, HF feeding, and diabetes and that infiltrating macrophages may be responsible for the activation of proinflammatory pathways (6, 23). Because FFAs are released in AT, we studied the effects of FFAs on AT macrophage function.

We first treated RAW264.7 murine monocyte/macrophage cells with a mixture of saturated and unsaturated FFAs and surveyed various stress/inflammatory signaling responses. FFA treatment broadly activated the JNK and IKKβ signaling path-

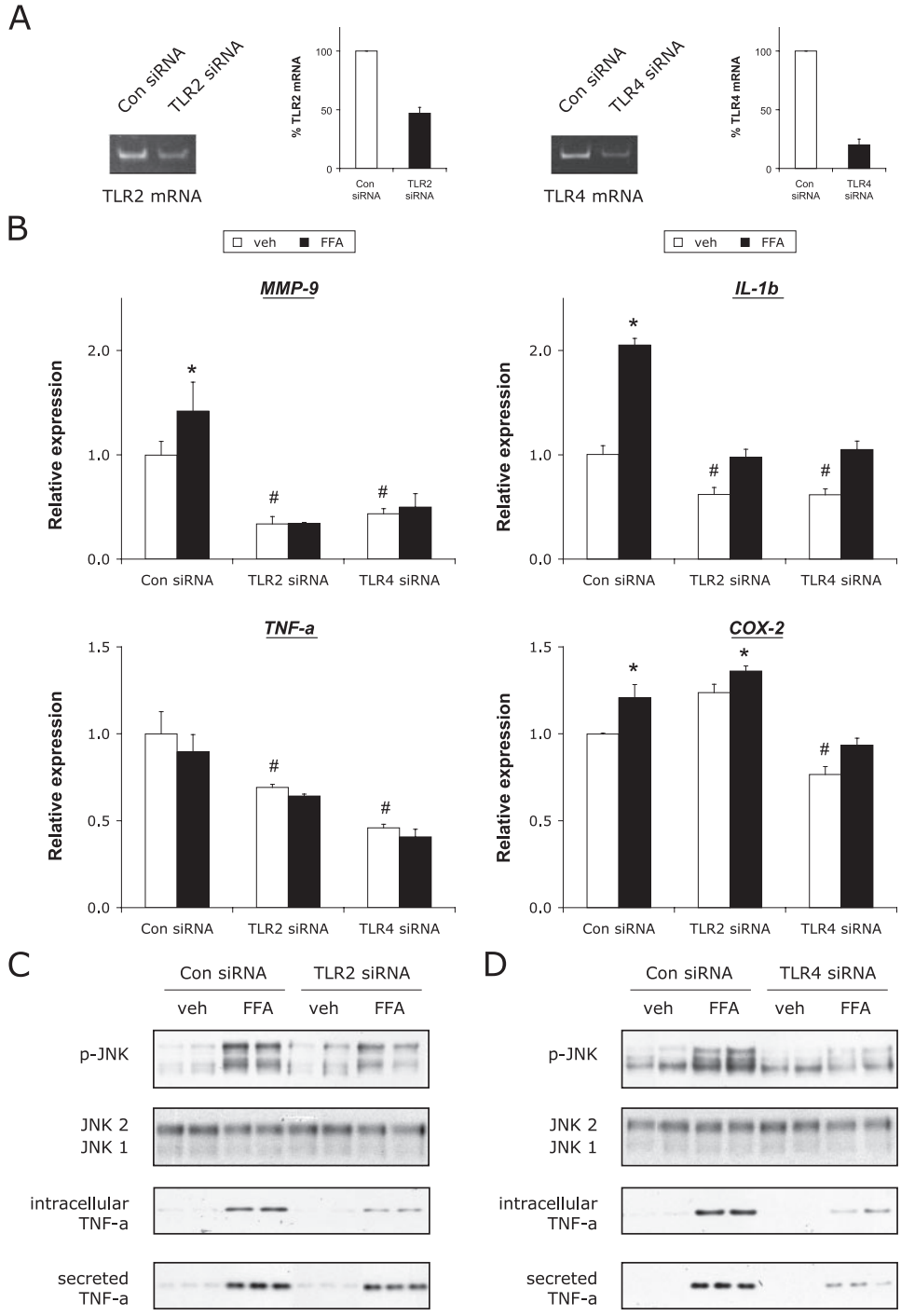

FIGURE 2. **TLR2 and TLR4 mediate FA signaling in RAW264.7 cells.** RAW264.7 cells were electroporated with siRNAs targeted against TLR2 or TLR4 or with control (*Con*) siRNA. 24–48 h post-electroporation, the cells were treated with 500 μM FFA or control vehicle (*veh*) for 3 h and harvested for real time qPCR and Western blot analyses. *A*, TLR2 and TLR4 KD efficiency in RAW264.7 cells. KD was visualized by gel electrophoresis of RT-PCR product, and KD efficiency was quantitated by real time qPCR. $n = 4$. *B*, effect of TLR2 and TLR4 KD on gene expression. TLR2 and TLR4 KD decreased basal expression of MMP-9 gene by >60% and of IL-1β gene by ~40%. TLR2 and TLR4 depletion also decreased TNF-α gene expression by ~30 and 55%, respectively, and TLR4 KD inhibited COX-2 gene basal expression by ~20%. In addition, TLR2 and TLR4 KD inhibited the FFA-induced increase in MMP-9 and IL-1β gene expression. *C* and *D*, both TLR2 KD and TLR4 KD inhibited the FFA-induced JNK phosphorylation and increase in intracellular and secreted TNF-α cytokine. This inhibition was more pronounced with TLR4 depletion. $n = 3$ or more in triplicate. *, $p < 0.05$ for FFA *versus* vehicle; #, $p < 0.05$ for vehicle *versus* control siRNA vehicle.

ways (Fig. 1*A*), in a time- and concentration-dependent manner, with JNK activation being observed as early as 5 min after FFA treatment (data not shown). After washing to remove FFAs, followed by a 12-h recovery period, inflammatory markers returned to base-line levels, and the cells were once again responsive to lipopolysaccharide stimulation (data not shown). Thus, the proinflammatory effects of FFAs were specific and reversible and did not result from cell toxicity. When the cells were treated with 500 μM FFA for 3 h, we observed induction of the proinflammatory genes IL-1β, IL-6, MCP-1, and MMP-9, an increase in intracellular MCP-1 and TNF-α levels, and an increase in secreted proinflammatory chemo/cytokines IL-1β, IL-6, MCP-1, and TNF-α (supplemental Fig. S1, *A–C*). When we tested individual FAs, each FA in the mixture, except for myristic acid, was able to activate the proinflammatory kinase pathways in RAW264.7 cells and increased intracellular and secreted TNF-α levels, albeit to different degrees (supplemental Fig. S1, *D* and *E*). Overall, the unsaturated FA arachidonic acid was most potent in causing these effects. We assessed whether a TZD, rosiglitazone, could inhibit FFA-induced inflammation in RAW264.7 cells and found that all the FFA-induced effects were attenuated by pretreatment with rosiglitazone (supplemental Fig. S2, *A–C*).

Contribution of JNK and IKKβ-NFκB to the FFA Proinflammatory Effects—Previous reports have documented that FFAs induce mostly NFκB-dependent effects, and we observed that FFA treatment activated both JNK and IKKβ signaling pathways. Therefore, we assessed the contribution of these two kinases to the overall FFA effect using siRNAs targeted specifically against JNK1, JNK2, and p65-NFκB. JNK1 and JNK2 siRNAs decreased levels of both JNK protein isoforms by >70% (13), and p65-NFκB siRNA decreased p65 protein levels by ~75% (Fig. 1*B*). JNK knockdown (KD) significantly reduced basal MMP-9, IL-1β, TNF-α, and COX-2 gene expression levels, and inhibited the FFA-induced up-regulation in IL-1β and MMP-9 gene expression (Fig. 1*C*). In contrast, knocking down p65 produced smaller inhibitory effects

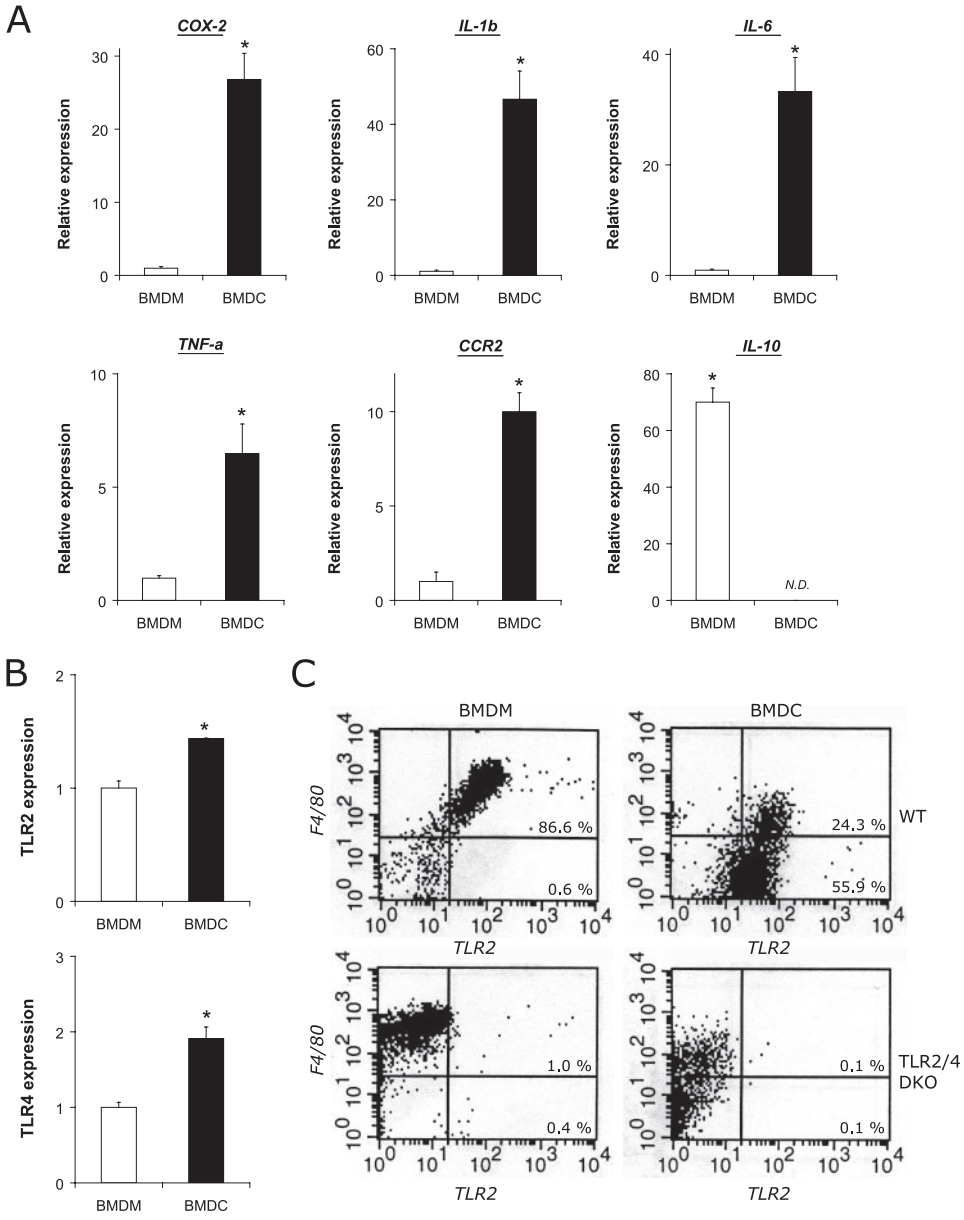

FIGURE 3. **Characteristics of bone marrow-derived cells.** Bone marrow cells were isolated from mouse tibias and femurs and differentiated into BMDMs and BMDCs, as described in detail under "Experimental Procedures." *A*, basal gene expression in BMDMs and BMDCs. The expression profiles from BMDMs and BMDCs are distinct. BMDCs, and not BMDMs, express high levels of the proinflammatory genes COX-2, IL-1β, IL-6, TNF-α, and CCR2. In contrast, BMDMs and not BMDCs, express high levels of anti-inflammatory gene IL-10. $n = 4$ or more in duplicate. *, $p < 0.05$. *B*, TLR2 and TLR4 gene expression levels are higher in BMDCs than BMDMs. RNA was extracted from BMDMs and BMDCs for semi-quantitative RT-PCR analysis. *C*, BMDMs and BMDCs express TLR2 at the cell surface. FACS logarithmic dot plots show that >80% of BMDMs and BMDCs express TLR2. BMDMs and BMDCs from TLR2/4 DKO mice did not display cell surface TLR2 protein.

on gene expression. Moreover, JNK KD resulted in decreased FFA-induced intracellular and secreted TNF-α levels (Fig. 1*D*), whereas p65 KD, while having the expected effect to decrease phosphorylation of NFκB, had little or no effect on intracellular and secreted TNF-α (Fig. 1*E*). This suggested that JNK plays a more central role in mediating the FFA-induced proinflammatory effects in RAW264.7 cells. We thus focused on examining the role of JNK kinase in mediating the effects of FFAs.

TLR2 and TLR4 Mediate FA Signaling in RAW264.7 Cells—TLRs are expressed on monocytes and macrophages, and it has been reported that bacterial lipopolysaccharide, which contains an FA moiety, can induce proinflammatory effects through TLR4 (17, 24, 25). Thus, we hypothesized that TLR4, and possibly TLR2, another member of the TLR family, could mediate the FFA proinflammatory signals. To test this idea, siRNAs were used to knockdown TLR4 and TLR2 proteins in RAW264.7 cells (Fig. 2*A*), achieving ~50% and ~75% KD efficiency for TLR2 and TLR4, respectively (*bar graph* in Fig. 2*A*). TLR2 KD significantly reduced basal expression of MMP-9, IL-1β, and TNF-α genes, whereas TLR4 KD reduced the basal expression of these genes and that of COX-2 (Fig. 2*B*). TLR2 and TLR4 KD also inhibited the FFA-induced up-regulation in IL-1β and MMP-9 gene expression. Fig. 2*C* shows that in the TLR2 KD cells, FFA-induced JNK phosphorylation was inhibited, as was the increase in intracellular and secreted TNF-α levels. When TLR4 was depleted, these proinflammatory responses were also inhibited, but to a greater extent (Fig. 2*D*). These results indicate that both TLR4 and TLR2 play a role in mediating FA signaling via JNK activation.

Studies in Bone Marrow-derived Cells—RAW264.7 cells have been extensively used as a model cell line for studies of macrophage biology. We found that RAW264.7 cells express high levels of the macrophage and myeloid cell surface markers F4/80 and CD11b but also high levels of a cell surface marker more typical of dendritic and T cells, CD11c (data not shown). With this in mind, and given the heterogeneity and plasticity of the macrophage population, we further examined the effects of FFAs in two types of primary myeloid-derived cell types: BMDMs, which express F4/80, CD11b but not CD11c, and BMDCs, which express all three markers. BMDMs and BMDCs were prepared as described in detail under "Experimental Procedures." According to previously established methods, the phenotype of these primary cells was confirmed by FACS using fluorescently labeled antibodies showing that BMDMs express F4/80 and CD11b, whereas BMDCs are positive for F4/80, CD11b, and CD11c (data not shown).

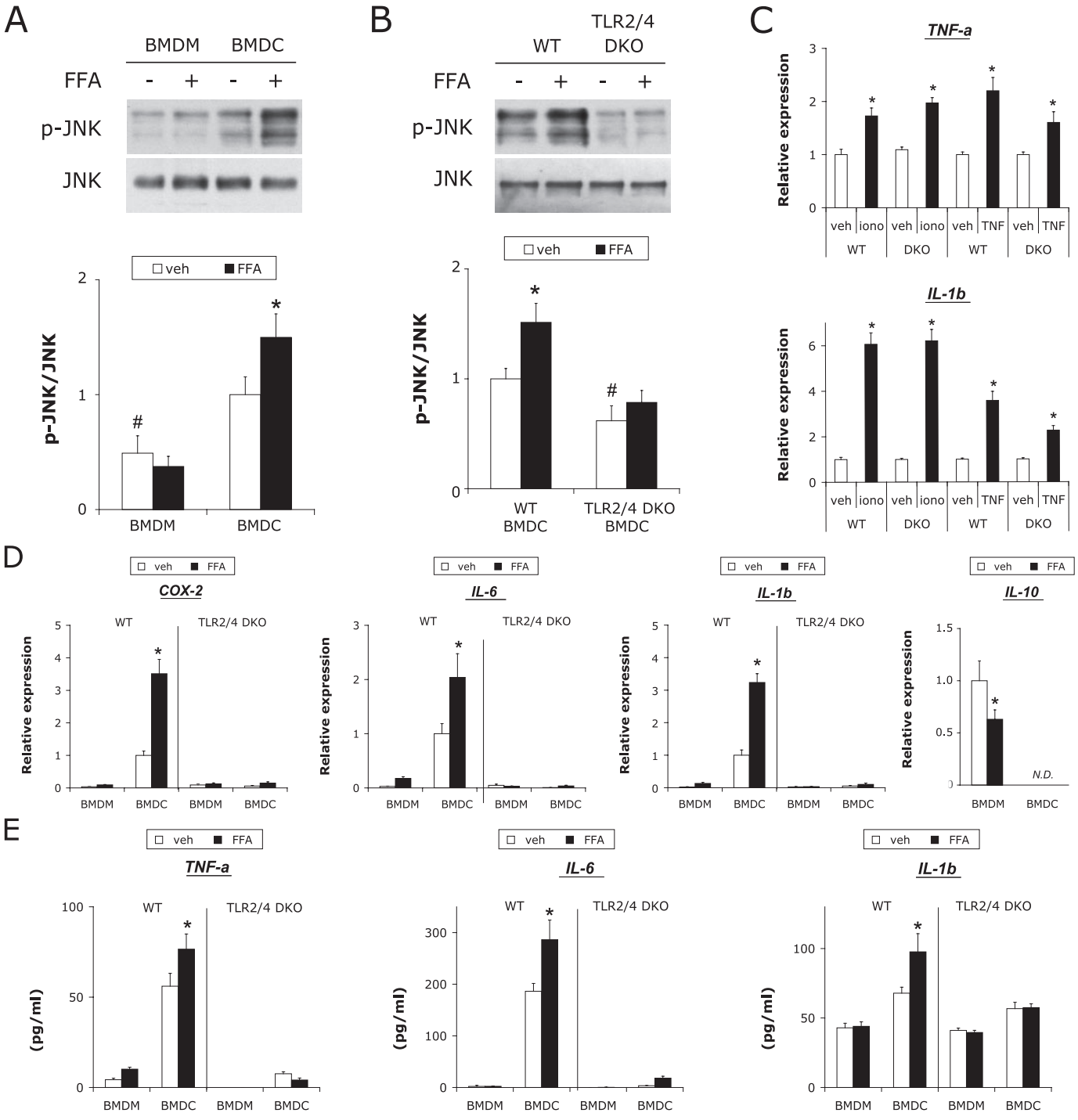

FIGURE 4. **FFAs induce inflammation in BMDCs but not in BMDMs.** *A*, FFAs increase JNK phosphorylation in BMDCs but not BMDMs. WT BMDMs and BMDCs were treated with 500 μM FFA or vehicle control (*veh*) and JNK phosphorylation was assessed by immunoblotting. Basal p-JNK levels were ~50% lower in BMDMs than BMDCs. FFA treatment increased p-JNK levels in BMDCs (by ~33%) but not in BMDMs. p-JNK levels were normalized against total JNK protein and quantification of six independent experiments is presented in the bar graph. *B*, FFAs increase JNK phosphorylation in WT BMDCs and not TLR2/4 DKO BMDCs. BMDCs from WT and TLR2/4 DKO mice were treated and analyzed as above. Quantification of four independent experiments (with duplicates) is presented in the bar graph. *C*, TLR2/4 DKO BMDCs do not respond to FFAs specifically but these cells are not broadly hyporesponsive cells as they can be activated by other treatments. Treatment of TLR2/4 DKO BMDCs with 10 ng/ml TNF-α (*TNF*) and 1 μg/ml ionomycin (*iono*) markedly increased TNF-α and IL-1β proinflammatory gene expression in those cells, similar to what is observed in treated WT BMDCs. *D*, effect of FFAs on BMDM and BMDC gene expression profiles. BMDMs and BMDCs were prepared from WT (*left panels* of bar graphs) and TLR2/4 DKO (*right panels* of bar graphs) mice and treated with 500 μM for 3 h prior to RNA extraction and real time qPCR analysis ($n = 4$ or more in duplicate). FFA treatment increased COX-2, IL-6, and IL-1β gene expression by 3.5-, 2.0-, and 3.3-fold, respectively, in WT BMDCs and not in BMDMs. This FFA-induced up-regulation in gene expression was not observed in TLR2/4 DKO BMDCs. In addition, BMDMs but not BMDCs express anti-inflammatory IL-10 cytokine, and IL-10 expression in BMDMs is decreased by FFA treatment. *E*, effect of FFAs on BMDM and BMDC cytokine secretion. CM was harvested from WT and TLR2/4 DKO BMDM and BMDC cultures treated with 500 μM FFA or vehicle control. Secreted TNF-α, IL-6, and IL-1β protein in CM was measured by ELISA. FFA treatment increased TNF-α, IL-6, and IL-1β levels by 32, 54, and 30%, respectively, in WT BMDCs. There is no significant effect of FFA treatment on TNF-α, IL-6, and IL-1β secretion in WT BMDMs. Furthermore, FFA treatment did not have a significant effect in BMDCs from TLR2/4 DKO mice. $n = 3$ with eight samples/condition. *, $p < 0.05$ for FFA (or other treatment) *versus* vehicle and for BMDC *versus* BMDM; #, $p < 0.05$ for BMDM or DKO BMDC *versus* WT BMDC.

A

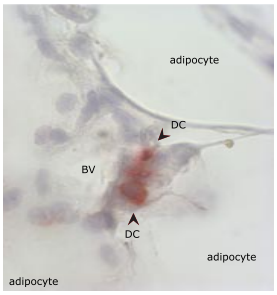

B

	WT	ob/ob
% F4/80-positive cells	35.1 ± 1.1	50.5 ± 2.3 *
Body weight (g)	27.23 ± 0.32	44.80 ± 3.66 *
Epididymal fat pad weight (g)	0.60 ± 0.02	2.96 ± 0.39 *
# of mice	3	4

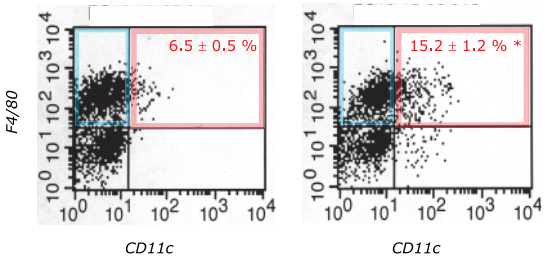

C

	1-wk NC	1-wk HFD	12-wk NC	12-wk HFD
% F4/80-positive cells	38.4 ± 0.6	42.5 ± 2.2	46.6 ± 2.7	56.1 ± 2.3 *
Body weight (g)	28.43 ± 0.70	29.57 ± 0.94	30.08 ± 1.45	34.16 ± 0.99 *
Epididymal fat pad weight (g)	0.51 ± 0.05	0.80 ± 0.09 *	0.81 ± 0.12	1.44 ± 0.12 *
# of mice	9	7	5	5

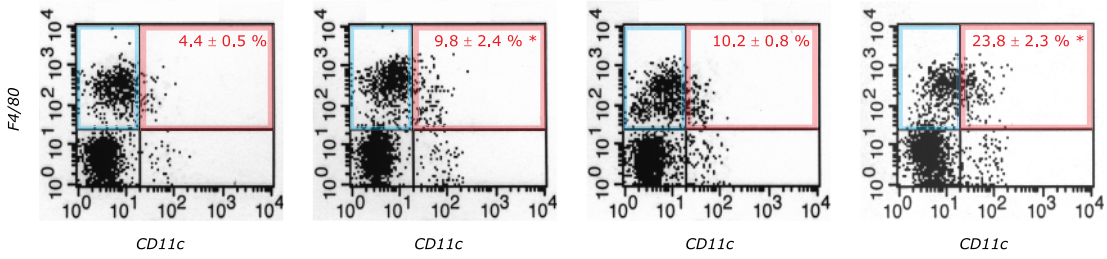

D

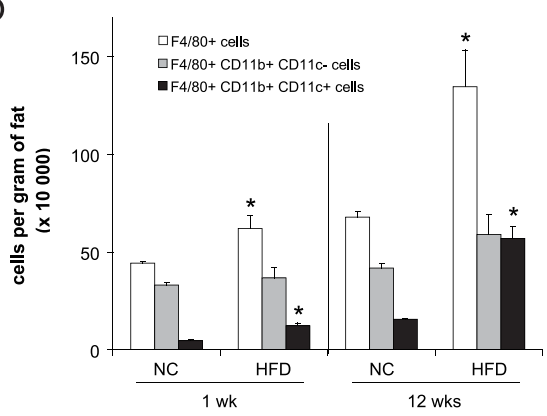

E

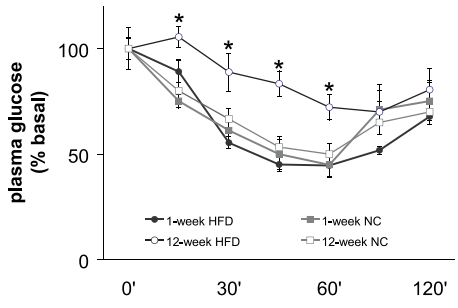

F

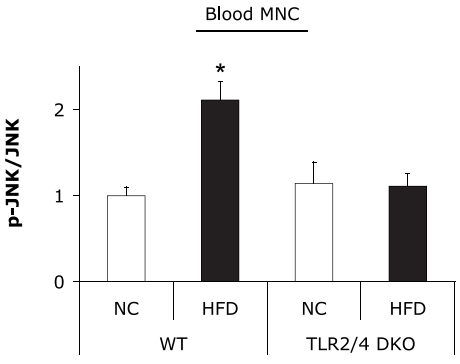

G

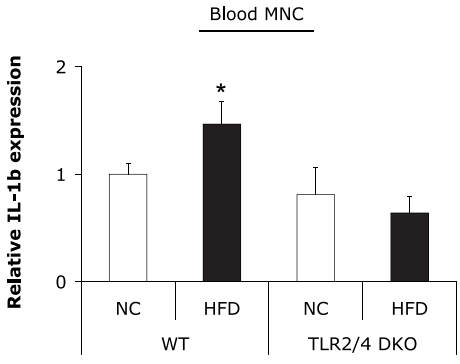

To characterize these two cell types, we examined the expression of inflammatory genes by qPCR (Fig. 3*A*). The relative expression of COX-2, CCR2, IL-1β, IL-6, and TNF-α genes was strikingly higher in BMDCs than BMDMs ($p <$ 0.05 or less), suggesting that BMDCs possess greater proinflammatory activity than BMDMs. Consistent with this, BMDMs expressed high levels of anti-inflammatory cytokine IL-10, whereas BMDCs exhibited no detectable levels of IL-10. BMDMs and BMDCs have been shown to express TLR2 and TLR4. Because BMDCs have heightened proinflammatory activity and because FFAs exert their inflammatory effects through both TLR2 and TLR4, we determined whether BMDCs and BMDMs differentially express TLR2 and TLR4. As shown in Fig. 3*B*, both cell types expressed TLR2 and TLR4 mRNA, with higher levels of expression in BMDCs. FACS analysis showed that >80% of BMDMs and BMDCs expressed TLR2 on the cell surface (Fig. 3*C*, *upper panels*). We also analyzed BMDMs and BMDCs prepared from TLR2 and TLR4 double knock-out (TLR2/4 DKO) mice by FACS. As expected, BMDMs and BMDCs showed no TLR2 expression (*lower panels*). Because of limitations of FACS antibodies against mouse TLR4, we were unable to assess TLR4 cell surface expression.

FFAs Induce Inflammation in BMDCs but Not in BMDMs—We treated BMDMs and BMDCs with FFAs, and Fig. 4*A* shows that basal JNK phosphorylation is higher in BMDCs than BMDMs (*lane 3 versus lane 1*) and that FFA treatment further enhanced p-JNK levels in BMDCs but not in BMDMs (*lane 2 versus lane 1* and *lane 4 versus* 3). In agreement with our findings that both TLR2 and TLR4 mediate the effects of FFAs, we found that FFA treatment of BMDCs lacking both TLR2 and TLR4 did not increase p-JNK levels (Fig. 4*B*) in these cells. This further supports a critical role for JNK kinase in mediating the effects of FFAs. The lack of an inflammatory response in TLR2/4 DKO BMDCs was relatively specific to FFA stimulation, because treatment of these cells with ionomycin or exogenous TNF-α produced an increase in proinflammatory TNF-α and IL-1β gene expression comparable with that seen in WT BMDCs (Fig. 4*C*).

The effects of FFAs on inflammatory gene expression and cyto/chemokine secretion were compared between vehicle- and FFA-treated BMDMs and BMDCs (Fig. 4, *D* and *E*). Fig. 4*D* (*left panels* of *bar graphs*) shows that FFA treatment significantly increased COX-2, IL-6, and IL-1β gene expression in BMDCs and not in BMDMs. Furthermore, FFA treatment down-regulated the level of anti-inflammatory IL-10 gene expression in WT BMDMs, but not in BMDCs. In cells from TLR2/4 DKO mice, we found that BMDCs showed much lower basal COX-2, IL-6, and IL-1β gene expression profiles, with no significant effect of FFAs (Fig. 4*D*, *right panels* of *bar graphs*). ELISA analysis of conditioned medium showed that FFA treatment significantly increased the secretion of IL-1β, IL-6, and TNF-α cytokines from BMDCs and not BMDMs (Fig. 4*E*, *left panels*). This increase was abolished in TLR2/4 DKO BMDCs (Fig. 4*E*, *right panels*). This is consistent with the view that FFAs stimulate BMDCs via a TLR2/4-dependent mechanism. Pretreatment of the BMDCs with rosiglitazone attenuated the FFA-induced inflammation in BMDCs (supplemental Fig. S2*D*).

Studies of AT Macrophages—Our results have demonstrated that F4/80$^+$CD11b$^+$CD11c$^+$ BMDCs, and not F4/80$^+$CD11b$^+$-CD11c$^-$ BMDMs, are important target cells for FFAs. This raised the question as to whether triply positive F4/80$^+$CD11b$^+$-CD11c$^+$ cells reside in AT *in vivo*. We assessed the presence of these cells in AT by immunohistochemical staining of AT tissue sections with an antibody against CD11c. CD11c$^+$ cells were readily detected in AT (Fig. 5*A*), and the CD11c staining was excluded from adipocytes and localized to cells surrounding adipocytes, in close proximity to endothelial cells and blood vessels.

To quantitate the proportion of F4/80$^+$CD11b$^+$CD11c$^+$ cells within AT, we prepared SVFs from AT of WT and ob/ob mice and analyzed them by FACS. The logarithmic dot plot of FACS data from representative 3-month-old WT and ob/ob mice is displayed in Fig. 5*B*. The frequencies reported (% ± S.E.) were derived from multiple experiments. FACS analysis revealed that of the total SVF cells (SVCs), there was a higher percentage of F4/80$^+$ cells in the ob/ob mice than in lean WT controls (50.5 *versus* 35.1%). When we gated for F4/80, CD11b, and CD11c, we found that AT-derived SVFs contained both triply positive F4/80$^+$CD11b$^+$CD11c$^+$ (Fig. 5*B*, *upper right quadrant*) and doubly positive F4/80$^+$CD11b$^+$CD11c$^-$ cells (*upper left quadrant*). In the ob/ob mouse AT, a higher percentage of the total SVCs were triply positive (15.2%), compared with only 6.5% in WT mice. There was a very large increase in the number of triply positive cells in the AT of ob/ob mice, ranging from 20- to 100-fold, depending on whether the data are expressed per gram of fat (20-fold) or per mouse (100-fold) (data not shown).

Next, we asked whether HF feeding can also affect AT F4/80$^+$CD11b$^+$CD11c$^+$ cell content. To study this, we placed 3-month-old WT mice on a 40% HFD or low fat NC diet for 1 week and 12 weeks. Fig. 5*C* shows that HF feeding increased the

FIGURE 5. **Characterizing immune cell subpopulations in AT-derived SVFs.** *A*, AT contains resident CD11c$^+$ immune cells (denoted by *arrows*). Immunohistological analysis shows staining for CD11c antigen (shown in *red*). BV: blood vessel. *B*, ob/ob mice have elevated content in total F4/80$^+$ cells as well as in F4/80$^+$CD11b$^+$CD11c$^+$ triply positive cells compared with WT mice. Epididymal fat pads were extracted from 3-month-old male mice for SVF isolation. SVCs were stained for F4/80, CD11b, and CD11c cell surface proteins and analyzed by FACS. *C*, HFD increases F4/80$^+$ cell and triply positive cell content in AT. 3-month-old male mice were placed on a HFD or low fat NC for 1 or 12 weeks. At the end of the feeding study, animals were sacrificed and AT SVFs were isolated for FACS analysis. *D*, the increase in triply positive cells accounts for the majority of the increase in total F4/80$^+$ cells. The numbers of cells of F4/80$^+$ cells, doubly positive (F4/80$^+$CD11b$^+$CD11c$^-$), and triply positive cells were calculated from FACS data and SVF cell counts and expressed per gram of epididymal fat tissue. *E*, 1-week HF feeding does not cause insulin resistance that is measurable by ITT. After 1 or 12 weeks of HFD or NC, the mice were fasted for 6 h and subjected to ITT (0.6 units of insulin/kg of body weight; $n = 10$ for each group). No significant difference was observed between the two groups in the ITT time course after 1 week of HFD. However, HFD mice became insulin-resistant after 12 weeks of HFD. *F* and *G*, HF feeding rapidly increases the inflammatory status of blood mononuclear cells (MNC). MNC were harvested from WT and TLR2/4 DKO mice after 3 or 7 days (not shown) of HFD and subjected to immunoblotting and real time PCR analysis. *F*, 3-day HF feeding increases p-JNK levels in MNC from WT but not TLR2/4 DKO animals. *G*, 3-day HF feeding increases IL-1β proinflammatory cytokine expression in WT but not TLR2/4 DKO MNC. $n = 5$ or more. *, $p < 0.05$.

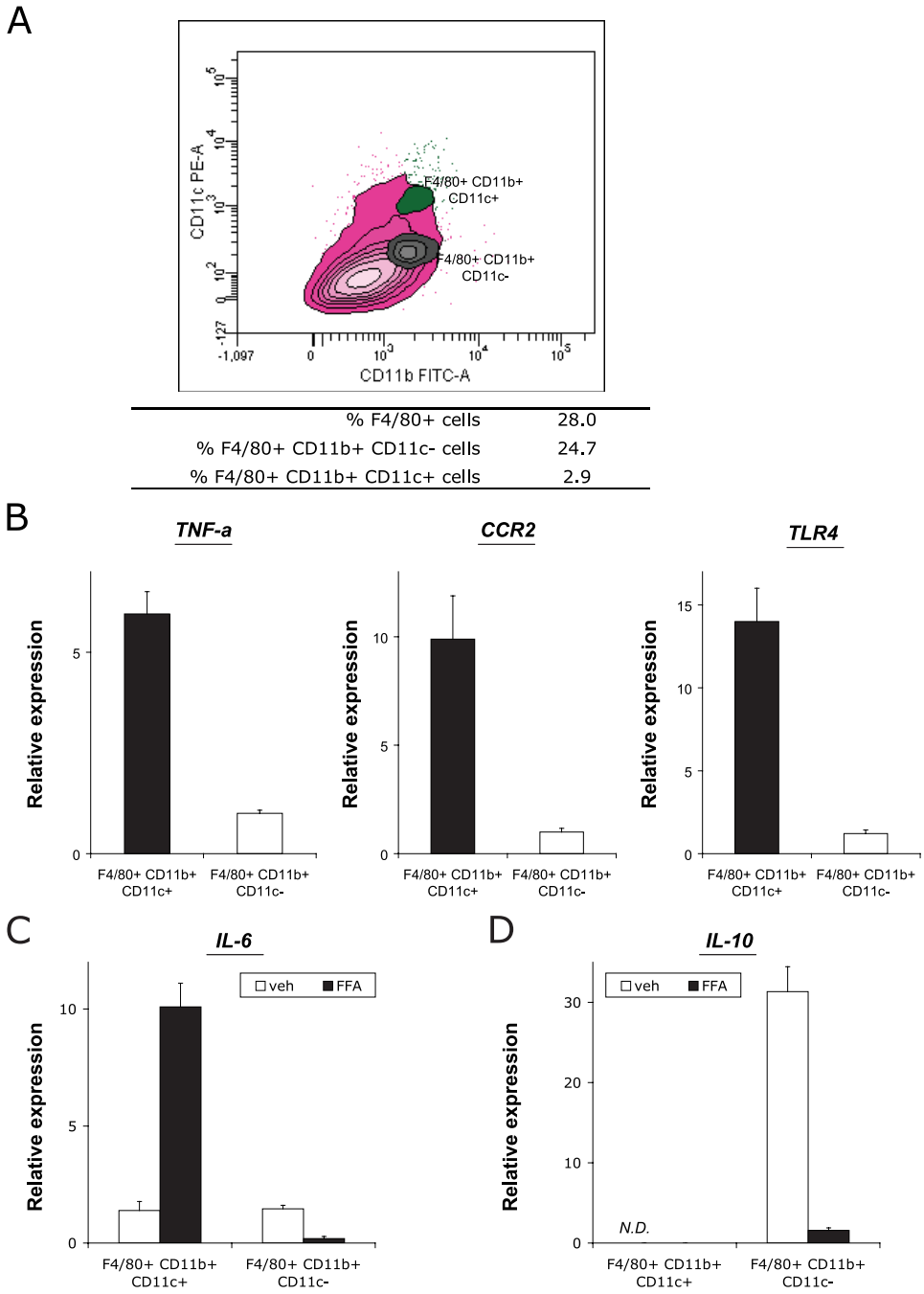

FIGURE 6. **F4/80$^+$CD11b$^+$CD11$^+$ cells in AT are activated by FFAs.** *A*, contour plot. Epididymal fat pads were dissected from twenty-five 3-month-old lean WT mice. SVFs were isolated and SVCs were sorted into two cell subpopulations, F4/80$^+$CD11b$^+$CD11$^-$ (shown in *brown*) and F4/80$^+$CD11b$^+$CD11$^+$ (shown in *green*) cells. *B*, triply positive cells express more proinflammatory markers than doubly positive cells. Real time qPCR analysis shows that triply positive cells express more TNF-α, CCR2, and TLR4 than doubly positive cells. *C* and *D*, FFA treatment increases IL-6 expression in F4/80$^+$CD11b$^+$CD11c$^+$ cells and decreases IL-10 expression in F4/80$^+$CD11b$^+$CD11c$^-$ cells. Sorted cells were treated with control vehicle or 500 μM FFAs for 3 h, and RNA was isolated for qPCR analysis.

percentage of F4/80$^+$ cells in SVFs after 1 and 12 weeks ($p < 0.05$). When cells were gated for F4/80, CD11b, and CD11c, the percentage of triply positive cells in SVFs increased by ~2.2-fold after 1 and 12 weeks of HFD ($p < 0.05$). The number of triply positive cells/gram of fat tissue increased by 2.6- and 3.6-fold after 1 and 12 weeks of HFD, respectively (Fig. 5*D*). As shown, upon HF feeding, the majority of the increase in F4/80$^+$ cells is due to the increase in triply positive and not doubly positive cells.

We found that HFD led to an increase in AT F4/80$^+$CD11b$^+$-CD11c$^+$ cells after just 1 week of HF feeding. At this time, mice had not gained a measurable amount of weight, and they were not yet insulin-resistant, unlike after 12 weeks of HFD, as assessed by ITT (Fig. 5*E*). This indicates that F4/80$^+$CD11b$^+$-CD11c$^+$ cell infiltration of AT can precede measurable insulin resistance and raises the question as to the source of these infiltrating cells. Based on reports showing that lipid infusion can trigger inflammation in mononuclear cells (MNC) in humans (26) and that a subset of blood monocytes with the potential to differentiate into CD11c$^+$ cells can be recruited to inflamed tissue sites (27), we hypothesized that the HFD-induced increase in mouse AT F4/80$^+$CD11b$^+$CD11c$^+$ cells correlates with an early increase in activated blood monocytes. We therefore probed the inflammatory status of blood MNC by examining p-JNK levels and the expression of IL-1β after 3 and 7 days of HFD. We found that p-JNK levels were significantly higher in MNC of 3- (Fig. 5*F*) and 7-day (data not shown) HF-fed mice compared with NC control mice. In contrast, MNC of mice lacking both TLR2 and TLR4 did not exhibit increased p-JNK levels induced by HF feeding. Consistent with this, blood MNC from 3- (Fig. 5*G*) and 7-day (data not shown) HFD mice expressed more IL-1β mRNA than cells from control animals, whereas MNC from TLR2/4 DKO mice did not show increased IL-1β expression when treated with FFAs. These data show that HFD can cause an increase in monocyte inflammation as early as 3 days after the beginning of the diet and support the idea that inflammation precedes and is conducive to the development of obesity and insulin resistance.

F4/80$^+$CD11b$^+$CD11c$^+$ Cells from AT Are Activated by FFAs—To characterize the macrophage subpopulations in normal mouse AT, doubly and triply positive cells were prepared from epididymal fat pads derived from twenty-five 3-month-old lean WT mice. SVCs were isolated and sorted into the two cell subpopulations of interest, F4/80$^+$CD11b$^+$CD11$^-$ and F4/80$^+$CD11b$^+$CD11$^+$ cells (Fig. 6*A*). The sorted cells were treated with control vehicle or FFAs followed by qPCR analysis.

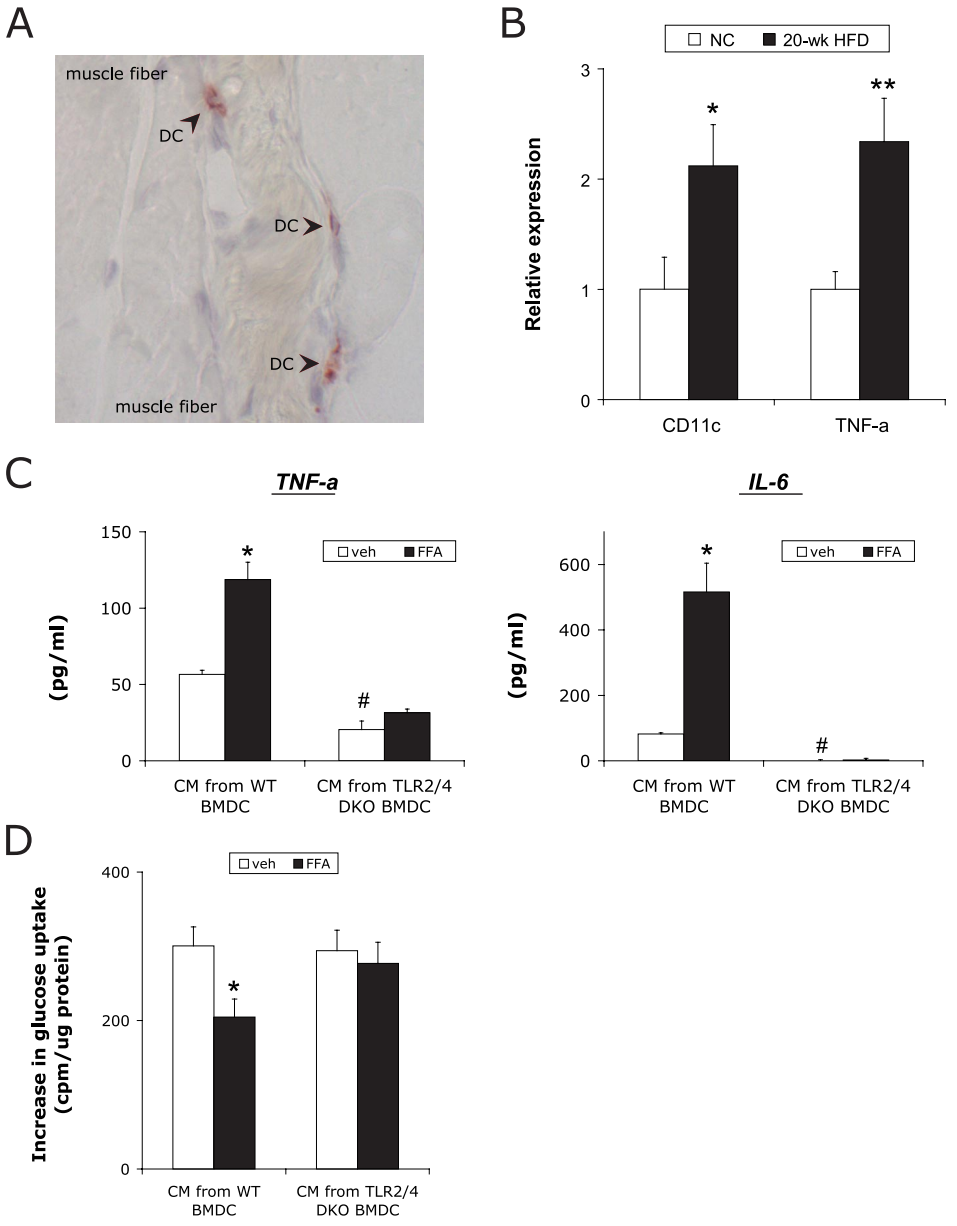

FIGURE 7. **CD11c$^+$ immune cells and insulin resistance in skeletal muscle cells.** *A*, CD11c$^+$ cells are present in skeletal muscle. Immunohistochemical analysis was performed on mouse skeletal tissue sections using an antibody against dendritic cell marker CD11c, revealing the presence CD11c staining (shown in *red*) in this tissue. *B*, HFD increases skeletal muscle CD11c and TNF-α expression. Soleus muscle was harvested from mice fed NC or HFD for 20 weeks and subjected to real time PCR analysis. $n = 3$ for each group. *C*, cytokine content in CM from BMDCs. CM was collected and analyzed, as described under "Experimental Procedures." CM from WT BMDCs contained high levels of TNF-α and IL-6, which were further increased by FFA treatment. CM from TLR2/4 DKO BMDCs contained much lower levels of those cytokines, which were not increased by FFA treatment. *D*, effect of BMDC CM on insulin-stimulated glucose uptake in L6 myotubes. Insulin (5 nM) increased glucose uptake in L6 cells co-incubated with vehicle-treated BMDC CM. This was significantly reduced when cells were co-incubated with CM from FFA-treated, activated BMDCs. This inhibition of the effect of insulin on glucose uptake was not present when cells were incubated with CM from FFA-treated BMDCs that lacked both TLR2 and TLR4. $n = 4$ in quadruplicates for each condition. *, $p < 0.05$; **, $p < 0.01$ for HFD/FFA *versus* NC/vehicle and insulin *versus* basal. #, $p < 0.05$ for CM-DKO BMDC *versus* CM-WT BMDC.

Fig. 6*B* shows that in the basal state, triply positive cells express more TNF-α, CCR2, and TLR4 than doubly positive cells. When cells were treated with FFAs, IL-6 gene expression was dramatically increased in triply but not doubly positive cells (Fig. 6*C*). Untreated doubly positive cells exhibited high levels of anti-inflammatory IL-10 mRNA expression, which was markedly decreased by FFA treatment (Fig. 6*D*). In contrast, triply positive cells did not express detectable levels of IL-10.

Effect of CD11c$^+$ Immune Cells on Skeletal Muscle Cell Insulin Sensitivity—To determine whether CD11c$^+$ cells are present in normal skeletal muscle, we performed immunohistochemical analysis of mouse skeletal tissue sections using an antibody against CD11c. CD11c-positive cells were detected, indicating that CD11c$^+$ immune cells are present in skeletal muscle (Fig. 7*A*). Expression of CD11c was measured in muscle tissue lysates from mice fed NC and HFD for 20 weeks, and Fig. 7*B* shows that muscle CD11c gene expression increases with HF feeding, as did TNF-α expression. These results prompted us to examine whether triply positive cells could play a role in promoting cellular insulin resistance.

To assess this, we measured the effect of conditioned medium (CM) harvested from BMDCs on insulin-stimulated glucose uptake in L6 myotubes. CM from WT and TLR2/4 DKO BMDCs were prepared as indicated. CM from FFA-treated WT BMDCs showed increased levels of secreted TNF-α and IL-6 compared with CM from vehicle-treated cells (Fig. 7*C*, *left panels* of *bar graphs*). As expected, CM from vehicle-treated TLR2/4 DKO BMDCs contained much less secreted TNF-α and no detectable IL-6, and most importantly, FFA treatment failed to stimulate TNF-α and IL-6 secretion (Fig. 7*C*, *right panels* of *bar graphs*). The results of the L6 myotube glucose uptake assays are presented in Fig. 7*D*. The net increase in glucose uptake was decreased ($p < 0.05$) in L6 cells incubated with CM from FFA-treated WT BMDCs compared with vehicle-treated BMDCs. As expected, when L6 cells were incubated with CM from TLR2/4 DKO BMDCs, the insulin effect on glucose uptake was not decreased by CM from FFA-treated cells.

DISCUSSION

The increase in macrophage infiltration and associated proinflammatory activity in hypertrophic and insulin-resistant AT first reported by Weisberg and Xu (4) has highlighted the role of macrophages in the development of obesity-associated insulin resistance(5, 6). Macrophages from adipose tissue were

found to express high levels of proinflammatory genes such as TNF-α, inducible nitric-oxide synthase, and IL-6, suggesting a causal link between inflammation and metabolic defects (23). This contention was strongly supported by myeloid-specific IKKβ gene deletion studies (9) and, more recently, by macrophage-specific CAP KO studies (28). All of these findings indicate that activation of inflammatory pathways in myeloid-derived immune cells contributes to the development of systemic insulin resistance.

In this study, we report that FFAs are important signaling molecules that can stimulate proinflammatory pathway activity in immune cells. Thus, treating RAW264.7 or BM-derived cells with a mixture of saturated and unsaturated FAs caused activation of the stress/inflammatory JNK and IKKβ signaling cascades, increased the expression of proinflammatory genes, and augmented the secretion of chemo/cytokines. In this regard, FFAs possess the capacity to induce stress/inflammatory signals in immune cells as reported in other cell types and tissues (1, 2, 13). We found that FAs signal through both TLR2 and TLR4 to activate immune cells. TLRs are essential participants in host defense against bacterial pathogens, but their role in nonmicrobial, sterile inflammatory processes is still being explored (20). Here we show that when TLR2 and TLR4 were knocked down in RAW264.7 cells or deleted in TLR2/4 DKO BM-derived cells, the FFA-induced inflammatory response was ablated, suggesting that both TLR2 and TLR4 deficiency in myeloid-derived cells contributes to the prevention of fat-induced insulin resistance. This is supported by a recent study showing that whole body TLR4 deficiency prevented insulin resistance in lipid-infused male mice (21, 29).

Our results provide novel evidence demonstrating that JNK activation is a key component in mediating TLR-dependent, nonmicrobial inflammation in immune cells. Interestingly, JNK activity is abnormally elevated in obesity, and JNK1 KO mice exhibit decreased adiposity and improved insulin sensitivity on a HFD (2). In light of our findings, it is possible that the protection from HFD-induced insulin resistance in JNK1 KO mice might originate from the inability of their macrophages to propagate JNK-dependent proinflammatory signals. Consistent with this, our recent studies show that macrophage-specific JNK1 KO mice are protected against HFD-induced insulin resistance.[3]

Pretreatment with rosiglitazone, a selective insulin sensitizing peroxisome proliferator-activated receptor γ ligand, inhibited the FFA-induced activation of the JNK inflammatory pathway in both RAW264.7 cells and BM-derived cells. This is consistent with previous studies demonstrating that TZDs have anti-inflammatory properties in various cell types (30–32) and suggests that the anti-inflammatory properties of TZDs in immune cells contributes to their insulin sensitizing effects.

We studied the effects of FFAs in two types of myeloid-derived cells: BMDMs and BMDCs, which are F4/80$^+$CD11b$^+$CD11c$^-$ and F4/80$^+$CD11b$^+$CD11c$^+$ cells, respectively. CD11c$^+$ BMDCs showed heightened proinflammatory activity, expressed more TLR2 and TLR4, and were activated by FFAs in contrast to CD11c$^-$ BMDMs. Interestingly, FFAs decreased IL-10 expression in BMDMs. Because IL-10 is highly expressed in AT macrophages from lean mice and can protect adipocytes from TNF-induced insulin resistance (33), these findings suggest that FFAs can induce insulin resistance via direct effects on immune cells to increase levels of cytokines that cause insulin resistance while decreasing levels of cytokines that prevent insulin resistance.

We found triply positive F4/80$^+$CD11b$^+$CD11c$^+$ and doubly positive F4/80$^+$CD11b$^+$CD11c$^-$ cells in mouse AT. In agreement with our data showing that CD11c$^+$ but not CD11c$^-$ cells (RAW264.7 cells and BMDCs *versus* BMDMs) respond to FFAs, we demonstrated that triply positive cells displayed increased proinflammatory markers compared with doubly positive cells and that FFA treatment enhanced inflammatory responses only in triply positive cells. Thus, AT contains at least two phenotypically distinct types of immune cells that respond differently to microenvironmental cues like FFAs. This further suggests that these cells fulfill different roles in AT homeostasis.

We show that acute and chronic HF feeding increased the number of F4/80$^+$ macrophages in AT. An increase in inflammatory markers and macrophage content in adipose tissue from obese rodents and humans has been previously reported (4, 5, 7, 8), but the increased number and nature of resident immune cells have largely been assessed by histological methods, with few (33–35) attempts to quantitate these findings. In the current studies, we used a quantitative approach, flow cytometry, to investigate the cell populations in AT-derived SVFs. Our FACS results clearly show that resident F4/80$^+$ and, more specifically, F4/80$^+$CD11b$^+$-CD11c$^+$ cell content increases under the influence of HFD and in genetic obesity. This is consistent with a recent report by Lumeng *et al.* (33) showing that ob/ob mice and mice rendered obese by a 20-week HFD exhibited increased F4/80$^+$ and F4/80$^+$CD11c$^+$ cell content in the SVFs. More interestingly, our results show that the most important changes induced by HF feeding are related to the shifts in immune cell subpopulations, with a significant increase in triply positive cells that contributes the major part to the increase in F4/80$^+$ total cell number. In addition, our results demonstrate that in contrast to doubly positive F4/80$^+$CD11b$^+$CD11c$^-$ cells, the F4/80$^+$CD11b$^+$CD11c$^+$ cells display elevated markers of proinflammatory gene activation and are responsive to the inflammatory effects of FFAs. Hence, these triply positive cells likely account for the enhanced proinflammatory activity reported in obese AT (4, 5, 7, 8). Moreover, because AT F4/80$^+$CD11b$^+$CD11c$^+$ cells can release cytokines, such as TNF-α, which stimulate lipolysis, this could raise the local tissue FFA concentrations, representing an interesting feed forward process that could contribute to sustained inflammation and the development of tissue insulin resistance.

We show that CD11c and TNF-α expression is increased in skeletal muscle of mice fed a HFD for 20 weeks, raising the possibility that activated CD11c$^+$ immune cells can promote cellular insulin resistance in this tissue. Consistent with this, we

[3] Solinas, G., Vilcu, C., Neels, J. G., Bandyopadhyay, G. K., Luo, J.-L., Naugler, W., Grivenikov, S., Wynshaw-Boris, A., Scadeng, M., Olefsky, J. M., and Karin, M. (2007) *Cell Metab.*, in press.

found that CM from FFA-activated, CD11c$^+$ BMDCs, but not CD11c$^-$ BMDMs (data not shown), inhibited insulin stimulated glucose uptake in L6 myotubes. Glucose uptake was not inhibited by CM from FFA-treated, TLR2/4-deficient BMDCs. These findings reinforce the role of TLR2 and TLR4 in mediating the effects of FFAs in myeloid cells and indicate that FA-responsive, CD11c$^+$ immune cells can directly modulate insulin sensitivity in insulin target cells.

The presence of F4/80$^+$CD11b$^+$CD11c$^+$ cells in AT raises the question as to the nature and origin of these cells. F4/80 and CD11c are primarily regarded as cell surface markers of macrophages and dendritic cells, which are immunophenotypically defined as F4/80$^+$CD11c$^-$ and F4/80$^-$CD11c$^+$, respectively. Thus, AT triply positive cells are unusual in that they have both macrophage- and dendritic cell-like features. These could be cells that have not yet completed their process of transitioning from a F4/80$^+$CD11c$^-$ to a F4/80$^-$CD11c$^+$ state or cells that have transitioned from a CD11c$^-$ to CD11c$^+$ phenotype but have retained some of their original phenotypical characteristics. For instance, they could be infiltrating F4/80$^+$ blood monocytes or AT resident F4/80$^+$ macrophages that have gradually acquired a CD11c$^+$ phenotype because of changes in the AT local microenvironment but have not yet, or not totally, lost F4/80 expression and macrophage properties. Interestingly, we found that AT F4/80$^+$CD11c$^+$ cells express high MHCII levels and DC-SIGN, another dendritic cell marker (data not shown), suggesting that at least some F4/80$^+$CD11b$^+$CD11c$^+$ cells may be functionally viewed as dendritic-like.

The increased content of AT triply positive cells in obesity and upon HFD further poses the question as to the source of these new cells. Do infiltrating cells derive from circulating monocytes that already display a CD11c$^+$ profile, or do they originate from invasive CD11c$^-$ resident tissue macrophages which undergo conversion to CD11c$^+$ cells because of local environmental cues? Our findings show that increased triply positive cell content in AT correlates with increased blood MNC activation. This suggests that activated MNC may be precursor cells for the F4/80$^+$CD11b$^+$CD11c$^+$ cells invading inflamed AT tissue and that analysis of the inflammatory status of circulating monocytes (36, 37) might prove to be a useful tool to gain insight into the development of obesity-associated insulin resistance.

In summary, we have provided a novel mechanistic link between lipid metabolism, inflammation, and insulin resistance. We showed that FFAs activate RAW264.7 and BMDCs via TLR2-, TLR4-, and JNK-dependent inflammatory pathways. CD11c$^+$ immune cells are the key targets for the proinflammatory actions of FFAs, as well as for the anti-inflammatory actions of TZDs, and acute and chronic HF feeding increases the number of F4/80$^+$CD11b$^+$CD11c$^+$ cells and their relative contribution to the total F4/80$^+$ cell number in AT. Thus, metabolic signals can utilize immune signaling mechanisms to trigger the activation of immune cells. Our findings support the view that FFA-induced, TLR-mediated activation of JNK proinflammatory pathways in CD11c$^+$ immune cells plays a central role in the development of AT inflammation and insulin resistance.

Acknowledgments—We thank Dr. Shizuo Akira (University of Osaka, Osaka, Japan) for the TLR2/TLR4 DKO mice. We thank D. Yoakum for technical help, E. J. Hansen and G. J. Lin for editorial assistance, and Drs. G. K. Bandyopadhyay, N.-W. Chi, P. Li, and D. M. Rose for scientific advice. At the Rebecca & John Moores UCSD Cancer Center, we thank the Flow Cytometry Resource and D. J. Young for assistance with FACS analysis and thank the Histology and Immunohistochemistry Resource (Laarni Gapuz) and Dr. N. Varki for scientific advice.

REFERENCES

1. Yuan, M., Konstantopoulos, N., Lee, J., Hansen, L., Li, Z. W., Karin, M., and Shoelson, S. E. (2001) *Science* **293,** 1673–1677
2. Hirosumi, J., Tuncman, G., Chang, L., Gorgun, C. Z., Uysal, K. T., Maeda, K., Karin, M., and Hotamisligil, G. S. (2002) *Nature* **420,** 333–336
3. Dandona, P., Aljada, A., and Bandyopadhyay, A. (2004) *Trends Immunol.* **25,** 4–7
4. Weisberg, S. P., McCann, D., Desai, M., Rosenbaum, M., Leibel, R. L., and Ferrante, A. W., Jr. (2003) *J. Clin. Investig.* **112,** 1796–1808
5. Xu, H., Barnes, G. T., Yang, Q., Tan, G., Yang, D., Chou, C. J., Sole, J., Nichols, A., Ross, J. S., Tartaglia, L. A., and Chen, H. (2003) *J. Clin. Investig.* **112,** 1821–1830
6. Bouloumie, A., Curat, C. A., Sengenes, C., Lolmede, K., Miranville, A., and Busse, R. (2005) *Curr. Opin. Clin. Nutr. Metab. Care* **8,** 347–354
7. Cancello, R., Henegar, C., Viguerie, N., Taleb, S., Poitou, C., Rouault, C., Coupaye, M., Pelloux, V., Hugol, D., Bouillot, J. L., Bouloumie, A., Barbatelli, G., Cinti, S., Svensson, P. A., Barsh, G. S., Zucker, J. D., Basdevant, A., Langin, D., and Clement, K. (2005) *Diabetes* **54,** 2277–2286
8. Bruun, J. M., Helge, J. W., Richelsen, B., and Stallknecht, B. (2006) *Am. J. Physiol.* **290,** E961–E967
9. Arkan, M. C., Hevener, A. L., Greten, F. R., Maeda, S., Li, Z. W., Long, J. M., Wynshaw-Boris, A., Poli, G., Olefsky, J., and Karin, M. (2005) *Nat. Med.* **11,** 191–198
10. Mantovani, A., Sica, A., and Locati, M. (2005) *Immunity* **23,** 344–346
11. Lai, L., Alaverdi, N., Maltais, L., and Morse, H. C. R. (1998) *J. Immunol.* **160,** 3861–3868
12. Wellen, K. E., and Hotamisligil, G. S. (2005) *J. Clin. Investig.* **115,** 1111–1119
13. Nguyen, M. T., Satoh, H., Favelyukis, S., Babendure, J. L., Imamura, T., Sbodio, J. I., Zalevsky, J., Dahiyat, B. I., Chi, N. W., and Olefsky, J. M. (2005) *J. Biol. Chem.* **280,** 35361–35371
14. Boden, G. (2002) *Curr. Opin. Clin. Nutr. Metab. Care* **5,** 545–549
15. Kraegen, E. W., Cooney, G. J., Ye, J. M., Thompson, A. L., and Furler, S. M. (2001) *Exp. Clin. Endocrinol. Diabetes* **109,** (Suppl. 2) S189–S201
16. Boden, G. (1997) *Diabetes* **46,** 3–10
17. Takeda, K., and Akira, S. (2005) *Int. Immunol.* **17,** 1–14
18. Liew, F. Y., Xu, D., Brint, E. K., and O'Neill, L. A. (2005) *Nat. Rev. Immunol.* **5,** 446–458
19. Guha, M., and Mackman, N. (2001) *Cell Signal.* **13,** 85–94
20. Lee, J. Y., Zhao, L., Youn, H. S., Weatherill, A. R., Tapping, R., Feng, L., Lee, W. H., Fitzgerald, K. A., and Hwang, D. H. (2004) *J. Biol. Chem.* **279,** 16971–16979
21. Shi, H., Kokoeva, M. V., Inouye, K., Tzameli, I., Yin, H., and Flier, J. S. (2006) *J. Clin. Investig.* **116,** 3015–3025
22. Spector, A. A., John, K., and Fletcher, J. E. (1969) *J. Lipid Res.* **10,** 56–67
23. Kolb, H., and Mandrup-Poulsen, T. (2005) *Diabetologia* **48,** 1038–1050
24. Poltorak, A., He, X., Smirnova, I., Liu, M. Y., Van Huffel, C., Du, X., Birdwell, D., Alejos, E., Silva, M., Galanos, C., Freudenberg, M., Ricciardi-Castagnoli, P., Layton, B., and Beutler, B. (1998) *Science* **282,** 2085–2088
25. Hoshino, K., Takeuchi, O., Kawai, T., Sanjo, H., Ogawa, T., Takeda, Y., Takeda, K., and Akira, S. (1999) *J. Immunol.* **162,** 3749–3752
26. Tripathy, D., Mohanty, P., Dhindsa, S., Syed, T., Ghanim, H., Aljada, A., and Dandona, P. (2003) *Diabetes* **52,** 2882–2887
27. Geissmann, F., Jung, S., and Littman, D. R. (2003) *Immunity* **19,** 71–82

28. Lesniewski, L. A., Hosch, S. E., Neels, J. G., de Luca, C., Pashmforoush, M., Lumeng, C. N., Chiang, S.-H., Scadeng, M., Saltiel, A. R., and Olefsky, J. M. (2007) *Nat. Med.* **13,** 455–462
29. Tsukumo, D. M., Carvalho-Filho, M. A., Carvalheira, J. B., Prada, P. O., Hirabara, S. M., Schenka, A. A., Araujo, E. P., Vassallo, J., Curi, R., Velloso, L. A., and Saad, M. J. (2007) *Diabetes* **56,** 1986–1998
30. Delerive, P., Fruchart, J. C., and Staels, B. (2001) *J. Endocrinol.* **169,** 453–459
31. Daynes, R. A., and Jones, D. C. (2002) *Nat. Rev. Immunol.* **2,** 748–759
32. Mohanty, P., Aljada, A., Ghanim, H., Hofmeyer, D., Tripathy, D., Syed, T., Al-Haddad, W., Dhindsa, S., and Dandona, P. (2004) *J. Clin. Endocrinol. Metab.* **89,** 2728–2735
33. Lumeng, C. N., Bodzin, J. L., and Saltiel, A. R. (2007) *J. Clin. Investig.* **117,** 175–184
34. Curat, C. A. (2006) *Diabetologia* **49,** 744–747
35. Brake, D. K., Smith, E. O., Mersmann, H., Smith, C. W., and Robker, R. L. (2006) *Am. J. Physiol.* **291,** C1232–C1239
36. Ghanim, H., Aljada, A., Hofmeyer, D., Syed, T., Mohanty, P., and Dandona, P. (2004) *Circulation* **110,** 1564–1571
37. Boschmann, M., Engeli, S., Adams, F., Gorzelniak, K., Franke, G., Klaua, S., Kreuzberg, U., Luedtke, S., Kettritz, R., Sharma, A. M., Luft, F. C., and Jordan, J. (2005) *Hypertension* **46,** 130–136

Metabolism and Bioenergetics:

A Subpopulation of Macrophages Infiltrates Hypertrophic Adipose Tissue and Is Activated by Free Fatty Acids via Toll-like Receptors 2 and 4 and JNK-dependent Pathways

M. T. Audrey Nguyen, Svetlana Favelyukis, Anh-Khoi Nguyen, Donna Reichart, Peter A. Scott, Alan Jenn, Ru Liu-Bryan, Christopher K. Glass, Jaap G. Neels and Jerrold M. Olefsky

J. Biol. Chem. 2007, 282:35279-35292.
doi: 10.1074/jbc.M706762200 originally published online October 4, 2007